Progress of Theoretical Physics, Vol. 62, No. 1, July 1979

Elastic Pion-Deuteron Scattering and Dibaryon Resonances

Kimiyo KANAI, Akira MINAKA,* Atsushi NAKAMURA**
and Hiroyuki SUMIYOSHI*

Department of Physics, Tokyo Metropolitan University, Tokyo 158
**Department of Physics, Kyushu University, Fukuoka 812*
***Department of Physics, Waseda University, Tokyo 160*

(Received February 9, 1979)

We show that effects of dibaryon resonances can be clearly seen in the data on the differential cross section of πd elastic scattering. Giving the formulation of the Glauber model with the resonance formation term in πd direct channel in detail and analyzing all the data presently available by this model, we find that at least two resonances are needed in πd direct channel in order to explain the data. One of them may be ${}^3F_3$ (2.25 GeV) state of two nucleons which was found at Argonne and the other has mass value around 2.5 GeV. The data are not enough to determine the spin-parity of the latter but 0^+ seems somewhat preferable. The branching ratios of the resonances into πd system are also given.

§ 1. Introduction

The theoretical discussion on the existence of dibaryon resonance is ample in literature.[1)~8)] There are not a few experimental evidences for its existence.[9)~11)] The work in this field has been much intensified especially by recent experiments using the polarized proton beam and target where the strong evidence of diproton states in ${}^3F_3$ and ${}^1D_2$ waves was reported.[11)~13)] We expect these dibaryon resonances to give a wealth of information about hadron physics, though the nature of the dibaryon resonances has not yet been clarified. The question whether the resonances should be treated as a system of six quarks or as that of nucleon and its isobar or as the threshold effect has been discussed but is left unsettled. It seems necessary to us that properties of the dibaryon resonances should be investigated not only in the pp elastic scattering but also in other processes. Since the dibaryon resonance ${}^3F_3$ has small elasticity, there remain many decay channels.

It is of particular interest to study the channels including deuteron which contains six quarks. The analysis of the coupling between dibaryon and deuteron might tell us the resemblance or the difference between them. The simplest of these processes is the pion deuteron elastic scattering. Other processes are less advantageous for the study of dibaryon resonances because the analysis depends on unconfirmed models, such as the Yao model[14)] for the reaction $\pi d \to pp$, which contain the triangle diagram and the results become highly model dependent.

In Ref. 15) we have pointed that the dibaryon resonances can affect the πd elastic scattering and in Ref. 16) we have shown that the features of the differential cross section of the scattering at 441 MeV/c can be explained as the effect of the dibaryon $^3F_3$. The aim of this paper is to give the detailed formula to treat πd elastic scattering when dibaryon resonances are present in the intermediate state and to show that there is very strong evidence for the existence of at least two resonances in this process by analyzing all the experimental data presently available.

The deuteron is usually thought of as a system which 'almost certainly consists of a neutron and proton'.[17] Taking the scattering of the pion off the neutron and/or the proton in the system as a background, we will analyze the dibaryon formation process. Many theoretical calculations have been proposed to describe the elastic scattering. Among them the easiest is the Glauber prescription[18)~22)] and any other more ambitious calculations[23] cannot give better fits to the present data than this model. It is easy in this model to employ the πN scattering amplitude including all the partial waves and to utilize well-established deuteron form factor. Though the Glauber theory is not expected to hold for low energy and large angle, it can reproduce the differential cross section data over the wide energy range and often over the entire solid angle. See, for example, Ref. 20) and Fig. 2 in this paper for πd elastic scattering. Without entering into discussion about this unexpected agreement, we take the Glauber amplitude as the reliable background for the dibaryon formation process.

We assume the s-channel helicity amplitude of the πd elastic scattering is given by

$$f_{\mu\nu}=f^G_{\mu\nu}+f^D_{\mu\nu}\,, \tag{1·1}$$

where $f^G_{\mu\nu}$ stands for the helicity amplitude calculated on the basis of the Glauber theory and $f^D_{\mu\nu}$ is the dibaryon formation amplitude in πd direct channel. The normalization of the amplitudes is chosen so that the unpolarized cross section is given by

$$d\sigma/d\Omega_{\rm cm}=\frac{1}{3}\sum_{\mu,\nu}|f_{\mu\nu}|^2\,. \tag{1·2}$$

The unitarization of the amplitude is not considered in this paper.

In § 2 we construct the Glauber amplitude in the spin state and transform it into the one in the helicity state to obtain $f^G_{\mu\nu}$. We present the dibaryon formation amplitude $f^D_{\mu\nu}$ using the Breit-Wigner formula in § 3. On the basis of the formula (1·1) we analyze the experimental data of the πd elastic scattering in § 4. Section 5 is devoted to conclusion and discussion.

§ 2. Glauber amplitude

In this section we will derive the s-channel helicity amplitude of the πd elastic scattering, $f^G_{\mu\nu}$, using the Glauber model.

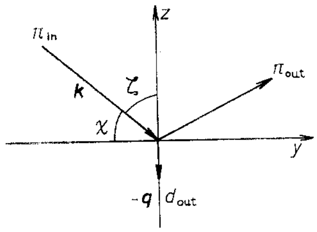

Fig. 1. Definition of the coordinate axes in the laboratory frame.

2.1. *Glauber amplitude in the spin state*

Here we use essentially the same amplitude as derived by Michael and Wilkin.[19] But in order to get the helicity amplitude, we have to recalculate it in more detail.

First we give the Glauber amplitude in the laboratory frame. The orientation of the axes is chosen as shown in Fig. 1. The momentum transfer $\boldsymbol{q}$ lies along the z axis, i.e., the quantization axis. In the Glauber theory the πd scattering amplitude is expressed as the sum of the single scattering term $T^{(1)}_{MM'}$ and the double scattering term $T^{(2)}_{MM'}$; they are given by

$$T^{(1)}_{MM'}(q)=\int d^3r\; e^{i\boldsymbol{q}\boldsymbol{r}/2}\Phi_M{}^*(\boldsymbol{r})\{F_{\pi p}(\boldsymbol{q})+F_{\pi n}(\boldsymbol{q})\}\Phi_{M'}(\boldsymbol{r}) \tag{2·1}$$

and

$$T^{(2)}_{MM'}(q)=\frac{i}{4\pi k}\int d^2\boldsymbol{q}'\;\mathcal{T}_{MM'}(\boldsymbol{q},\boldsymbol{q}'), \tag{2·2}$$

where

$$\begin{aligned}\mathcal{T}_{MM'}(\boldsymbol{q},\boldsymbol{q}')=\int d^3r\; e^{i\boldsymbol{q}'\boldsymbol{r}}\;\Phi_M{}^*(\boldsymbol{r})\Big[&F_{\pi n}\Big(\frac{\boldsymbol{q}}{2}-\boldsymbol{q}'\Big)F_{\pi p}\Big(\frac{\boldsymbol{q}}{2}+\boldsymbol{q}'\Big)\\ &+F_{\pi p}\Big(\frac{\boldsymbol{q}}{2}-\boldsymbol{q}'\Big)F_{\pi n}\Big(\frac{\boldsymbol{q}}{2}+\boldsymbol{q}'\Big)\\ &-F_{CEX}\Big(\frac{\boldsymbol{q}}{2}-\boldsymbol{q}'\Big)F_{CEX}\Big(\frac{\boldsymbol{q}}{2}+\boldsymbol{q}'\Big)\Big]\Phi_{M'}(\boldsymbol{r})\end{aligned} \tag{2·3}$$

with

$$F_{CEX}=[F_{\pi p}-F_{\pi n}]/\sqrt{2}\,. \tag{2·4}$$

The πN elastic scattering amplitudes, $F_{\pi p}$ and $F_{\pi n}$, take the form

$$F_{\pi N}(\boldsymbol{q})=a_{\pi N}(\boldsymbol{q})+\boldsymbol{\sigma}\cdot(\boldsymbol{q}\times\boldsymbol{Q})\,b_{\pi N}(\boldsymbol{q}), \tag{2·5}$$

in the laboratory frame, where $\boldsymbol{Q}$ is the mean of the incident and outgoing momenta of the pion and $a_{\pi N}$ and $b_{\pi N}$ are written in terms of the invariant amplitudes $A_{\pi N}$ and $B_{\pi N}$ as

$$a_{\pi N}(t)=\frac{m_N}{4\pi}\left(1-\frac{t}{4m_N{}^2}\right)^{1/2}\left(\frac{1}{s}\frac{\partial\Omega_{\rm cm}}{\partial\Omega_{\rm lab}}\right)^{1/2}A'_{\pi N}(t) \tag{2·6a}$$

and

$$b_{\pi N}(t)=\frac{i}{8\pi}\left(1-\frac{t}{4m_N{}^2}\right)^{-1/2}\left(\frac{1}{s}\frac{\partial\Omega_{\rm cm}}{\partial\Omega_{\rm lab}}\right)^{1/2}B_{\pi N}(t), \tag{2·6b}$$

where

$$A'_{\pi N}(t)=A_{\pi N}(t)-\frac{E_{\rm lab}+t/4m_N}{1-t/4m_N{}^2}B_{\pi N}(t). \tag{2·7}$$

s, t and $\Omega_{\rm cm}$ represent the square of the c.m. energy, the momentum transfer squared and c.m. solid angle of the πN system, respectively and m_N is the nucleon mass.

The deuteron wave function with the spin projection M is

$$\begin{aligned}\Phi_M(\boldsymbol{r})=&\frac{u(r)}{r}Y_{00}(\hat{r})C^{1/2\ 1/2\ 1}_{m_1\ m_2\ M}\chi^p_{m_1}\chi^n_{m_2}\\&+\frac{w(r)}{r}Y_{2,M-m_1-m_2}(\hat{r})C^{2\qquad\qquad 1\qquad\quad 1}_{M-m_1-m_2\ m_1+m_2\ M}\\&\times C^{1/2\ 1/2\ 1}_{m_1\ m_2\ m_1+m_2}\chi^p_{m_1}\chi^n_{m_2},\end{aligned} \tag{2·8}$$

where $C^{j_1\ j_2\ J}_{m_1\ m_2\ M}$ are the Clebsch-Gordan coefficients and $\chi^p_{m_1}$ and $\chi^n_{m_2}$ are proton and neutron Pauli spinors with spin projection m_1 and m_2. The S and D radial wave functions, $u(r)$ and $w(r)$, are chosen to be real and are normalized as

$$\int_0^\infty(u^2+w^2)dr=1. \tag{2·9}$$

The explicit forms of $T^{(1)}_{MM'}$ and $T^{(2)}_{MM'}$ are given in the Appendix.

In order to construct the πN invariant amplitudes, $A_{\pi N}$ and $B_{\pi N}$, we have used the results of phase shift analysis of both SACLAY and CMU-LBL, but we found that the results of our calculation using both analyses differ only slightly. We shall only report the results using the former analysis because it covers wider energy region than the latter.

It is not unambiguous to determine the energies at which the πN scattering takes place, because the target nucleons inside the deuteron are different from the free ones. Here we take the energies following Ref. 20):

$$E^{\pi N}=\frac{1}{m_N}\{[(n^2+m_\pi{}^2-t/4)(m_N{}^2-t/4)]^{1/2}-t/4\}, \tag{2·10}$$

where

$$n^2=\{4m_d{}^2k^2_{\rm lab}+t(2m_dE_{\rm lab}+m_d{}^2+m_\pi{}^2)\}/(4m_d{}^2-t). \tag{2·11}$$

Here $E_{\rm lab}$ and $k_{\rm lab}$ are the energy and the momentum of the pion in the laboratory frame and t stands for the momentum transfer squared in πd scattering. The pion mass and the deuteron mass are denoted by m_π and m_d, respectively.

For the deuteron form factor we use Reid's hard core wave function.[24] As a check we have also examined Humberstone's[19] and Moravcsik's fit to the Gartenhaus wave function.[25] We find that the result is not so sensitive to the choice of the wave functions.

2.2. *Glauber amplitude in the helicity state*

Now we transform the Glauber amplitudes in the laboratory frame given in § 2.1 to the s-channel helicity amplitudes, $f^G_{\mu\nu}(\theta, \phi)$, where the direction of the incident deuteron is chosen as z-axis and θ and ϕ are the polar and azimuthal angles of the recoiled deuteron in the c.m. system. The indices ν and μ represent the helicity of the incident and the recoiled deuteron, respectively. A simple calculation gives

$$f^G_{\mu\nu}(\theta, \phi) = \sum_{MM'} \langle \mu | L | M' \rangle \langle M' \ (T^{(1)} + T^{(2)}) | M \rangle \times \langle M | R | \nu \rangle | \partial \Omega_{\text{lab}} / \partial \Omega_{\text{cm}} |^{1/2}, \tag{2·12}$$

where

$$\langle \mu | L | M' \rangle = \sum_{\lambda} e^{-i\phi\mu} d_{\mu\lambda}(\zeta) \mathcal{D}^1_{\lambda M'}\left(\frac{\pi}{2}, -\pi, 0\right) \tag{2·13a}$$

and

$$\langle M | R | \nu \rangle = \mathcal{D}^1_{M\nu}\left(-\frac{\pi}{2}, \zeta, -\phi\right). \tag{2·13b}$$

The definition of the angle ζ is shown in Fig. 1.

§ 3. Dibaryon resonance formation amplitude

In this section given are the s-channel helicity amplitudes of the dibaryon resonance formation.

The helicity amplitudes have the following partial wave decomposition:

$$f^D_{\mu\nu} = \frac{1}{2p} \sum_J \sum_{LL'} [(2L+1)(2L'+1)]^{1/2} C^{L1J}_{0\mu\mu} C^{L'1J}_{0\ \nu\nu} \times \mathcal{D}^J_{\nu\mu}(\phi, \theta, -\phi) T^J_{LL'}, \tag{3·1}$$

where p is the momentum in the center-of-mass frame and J and L are the total spin and the orbital angular momentum of the πd system. By parity conservation the partial waves $T^J_{LL'}$ are divided into two classes, which respectively contain the amplitudes of the form $T^J_{J\pm1, J\pm1}$ (natural parity) and T^J_{JJ} (unnatural parity).

We parametrize the partial wave amplitudes as follows:

$$T^J_{LL'} = 2m_R B^L_{1/2} B^{1/2}_{L'} \Gamma_{\text{tot}} / (m_R{}^2 - s - i m_R \Gamma_{\text{tot}}), \tag{3·2}$$

where m_R is the mass of the dibaryon resonance and B_L is the branching ratio into L wave πd system. We take account of the threshold factor as

$$\Gamma_{\text{tot}}=\begin{cases}\Gamma_0(p/p^*)^{2l+1} & \text{for } p\leq p^*, \\ \Gamma_0 & \text{for } p>p^*,\end{cases} \tag{3·3}$$

where p^* is the value of p at the resonance energy and we put

$$l=\begin{cases}L & \text{for } L=L', \\ J & \text{for } L\neq L'.\end{cases} \tag{3·4}$$

Summing the Glauber amplitude (2·12) and the dibaryon formation amplitude (3·1), we get the total helicity amplitude (1·1).

§ 4. Comparison with experimental data

4.1. *Glauber model*

First the predictions from the Glauber model without dibaryon resonances are compared with the experimental angular distributions in the center-of-mass frame. The results are shown in Figs. 2~5 by dotted lines at the incident momenta between 245 and 895 MeV/c. The experimental data are taken from Refs. 26)~30). In the lower energy region, i.e., 245 and 290 MeV/c, the Glauber model reproduces the data quite well all over the angles. (See Figs. 2(a) and (b).) However, as incident energy increases, the significant deviation between the theory and experiment appears in the backward region. At 343 and 370 MeV/c, the calculated curves agree with the data in the forward direction but lie lower in the backward direction. In the case of 441 and 539 MeV/c, both the dip structure seen around 100° and backward enhancement cannot be reproduced by this model. At the incident momentum 637 MeV/c, the theoretical curve is lower than the data not only in the backward region but also in the forward region. Moreover it gives no sign of any dip structure as is shown in Fig. 5(a). As the energy

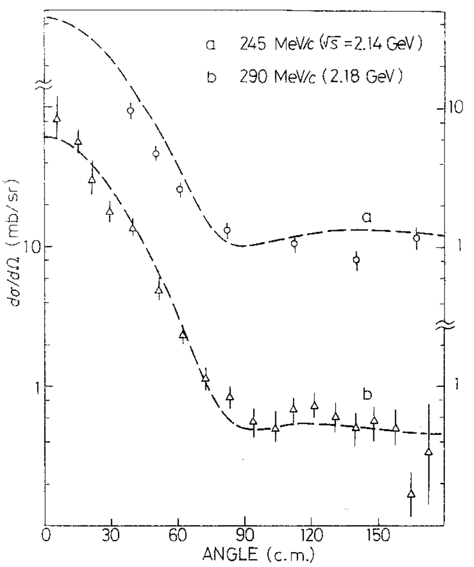

Fig. 2. The angular distributions of πd elastic scattering at (a) 245 MeV/c and (b) 290 MeV/c. The dashed lines show the results of the Glauber model. The introduction of the dibaryon resonances given in Table I little affects the results and then the cases are not shown. The data are taken from Refs. 26) and 27).

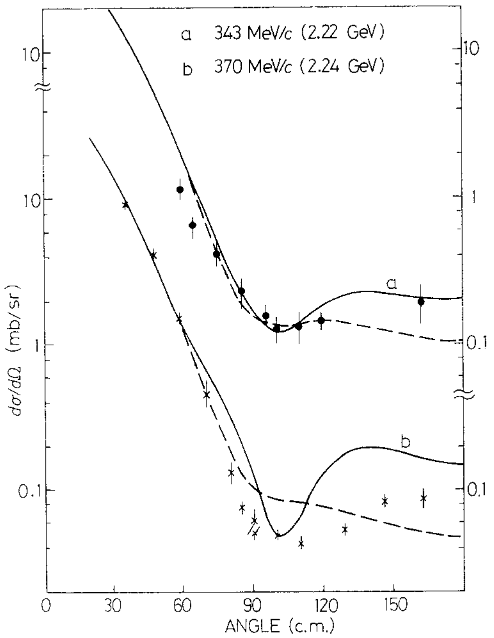

Fig. 3. The angular distributions of πd elastic scattering at (a) 343 MeV/c and (b) 370 MeV/c. The dashed lines show the results of the Glauber model, while the results with both resonances given in Table I are shown by the solid lines. Data are taken from Refs. 29) and 28).

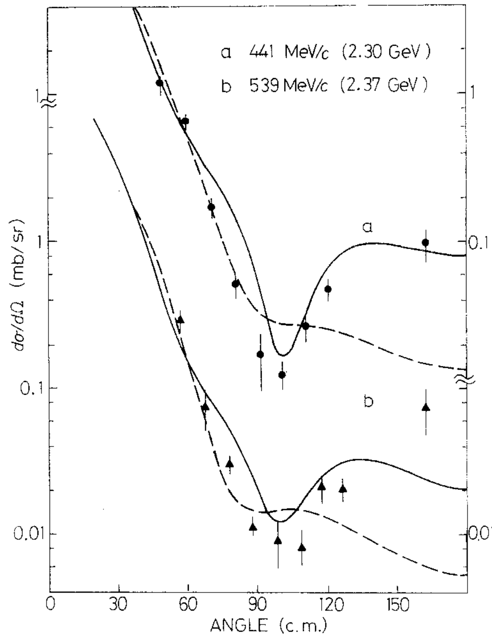

Fig. 4. Same as in Fig. 3 but at (a) 441 MeV/c and (b) 539 MeV/c. Data are taken from Ref. 29).

becomes higher, however, it can again reproduce the data rather well except for the angular region around 70°.

The outstanding disagreements are observed in the energy region $2.2 \lesssim \sqrt{s} \lesssim 2.6$ GeV where the recently reported dibaryon resonances exist. In Fig. 6, the calculated curve of the differential cross section at 180° is shown with the experimental data[9] as a function of the laboratory momentum of the incident π.

4.2. *Effect of dibaryon resonances*

We introduce the dibaryon resonances according to the formulation given in § 3. Each dibaryon resonance amplitude has five (or six) parameters; the mass m_R, the total width Γ_0, the spin J, the parity and the decay branching ratio (ratios) B_L into the πd system. After some trials we take two resonances whose parameters are given in Table I. The results are shown in Figs. 3~6 by solid lines.

First we discuss the effect of the $^3F_3$ resonance which was found in polarized pp scattering.[11] We have fixed the spin and parity and roughly estimated the values of mass and total width of this resonance following the results in Ref. 13).

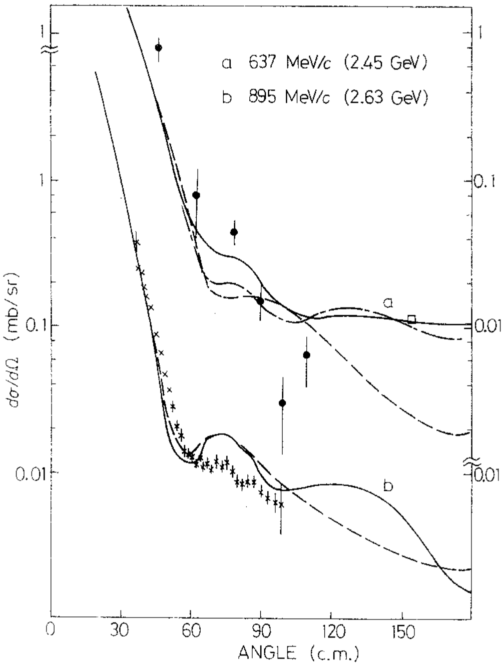

Fig. 5. Same as in Fig. 3 but at (a) 637 MeV/c and (b) 895 MeV/c. In Fig. (a) the result with the $J^P=3^-$ resonance is given by the dot-dashed line. Data are taken from Refs. 29), 9) and 30).

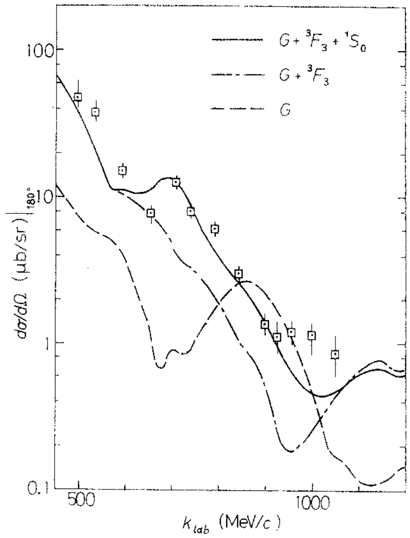

Fig. 6. The energy dependence of the differential cross-section at 180°. The meaning of the lines is the same as in Fig. 5 (a). Data are taken from Ref. 9).

Table 1. Resonance parameters

J^P	m_R(GeV)	Γ_0(GeV)	B_{J+1}	B_{J-1}
3^-	2.25	0.18	0.08	0.01
0^+	2.50	0.08	0.16	—

In the lower energy region, i.e., at 245 and 290 MeV/c, this resonance has little influence on the cross section as we have expected and the agreement with the data is still good. At 343 and 370 MeV/c there can be seen some improvements. (Strictly speaking, it is doubtful whether the agreement with the data at 370 MeV/c is really improved. There is, however, a controversy on the data[31] and we should be careful in extracting conclusions from the data at 370 MeV/c.) The effect of the dibaryon resonance ${}^3F_3$ is most pronounced at 441 and 539 MeV/c. The sharp dip structure around 100° and backward enhancement can be reproduced, though it shows a little discrepancy around 60~80°. Note that the experimental data at 448 MeV/c[32] is higher at this region. In the still higher energy region, it improves slightly but the backward enhancement is not sufficient at 637 MeV/c.

If we take the branching ratio into D wave πd system larger than that into G wave, the dip structure at 441 MeV/c cannot be reproduced. From the data on energy dependence of the differential cross section at $\theta_{cm}=180°$, shown in Fig. 6, we can safely say $100 \lesssim \Gamma_0 \lesssim 250$ MeV, though we need the data for lower energy in order to estimate the value more precisely. The prominent effect of this resonance is to produce a sharp dip structure only above the resonance energy. The sharp dip structure is observed at 441 MeV/c but not at 370 MeV/c. Then we can conclude that the mass of the resonance $^3F_3$ lies between 2.24 and 2.30 GeV.

With only the resonance $^3F_3$ included (the dot-dashed curve in Fig. 6), the shoulder structure around 700 MeV/c in the data on the energy dependence of the differential cross section at $\theta_{cm}=180°$ cannot be reproduced. Another resonance seems to be required around 2.5 GeV. The analysis of pp scattering also shows the existence of the resonance in this mass region which may be $^1G_4$ or $^1S_0$.[11),13)] We have examined all possible cases with $J \leqq 5$. We have determined total width and branching ratio to fit the data in Fig. 6 and compared the results with the differential cross section at 539 and 637 MeV/c. When there are two possible waves in πd system (natural parity with $J>0$), we have studied only three cases for each J; one of the branching ratios, B_{J+1} or B_{J-1}, does vanish or they are equal in magnitude. Though the available experimental data in the backward region around this energy is not enough to determine the spin and parity of this resonance decisively, we find the cases of 0^+ and 1^- are somewhat favorable. In Figs. 3~6 we present the results in the case of 0^+ by the solid lines. This resonance little affects the data below 539 MeV/c.

We also examined the resonance $^1D_2$ (2.17 GeV) reported in Refs. 11) and 13). This resonance is expected to affect the data in the region from 245 to 343 MeV/c. In this energy region, however, the Glauber model can reproduce the experimental data successfully over the whole angle. Therefore the branching ratio of $^1D_2$ into πd channel should be small; it may be at most 5%.

§ 5. Concluding remarks

Above the $\Delta(1232)$ resonance region, πN amplitudes include many partial waves. In this energy region, it is difficult to explain the observed deep and large dip of the πd differential cross section around 100° on the basis of multiple scattering formalism. We have presented the formalism which includes direct-channel resonance states with $I=1$, $B=2$. The theoretical calculation based on this formalism can reproduce the prominent feature of the experimental data, though the results around 600 MeV/c are far from satisfactory. The structure in the differential cross section at 180° was thought as the effect of the πN resonances,[33)] while our calculated curve without dibaryon resonances (the dashed line in Fig. 6) is far lower than the data. Though the Glauber calculation may be unsound at

180°, it may still give some reasonable results, because Faddeev type calculations, for example, show the results similar to those of the Glauber model even in the backward region.

We found that the dibaryon resonances have a large influence on πd scattering. Hence theories of πd scattering should take the existence of the dibaryon states into consideration. The differential cross sections are sensitive to parameters of the resonances; in this respect πd elastic scattering experiments are very advantageous for the examination of the dibaryon resonances.

In order to study characters of the resonances in much greater detail, both theoretical and experimental developments are required. More reliable model for the background provides more reliable results about the resonances. We have employed the Glauber model to calculate the background amplitudes, $f^{a}_{\mu\nu}$, while it is worth while calculating them on the basis of, for example, Faddeev type model. Needless to say, precise measurements to large angles are extremely valuable.

In this paper we have assumed the couplings between πd system and dibaryon resonance to be real, for simplicity. Generally speaking, they have imaginary parts due to unitarity. We will investigate effect of unitarity correction to the amplitudes in a forthcoming paper. (If one wants to analyze experimental data in a model independent way, the branching ratios may be treated as free complex parameters.)

Experiments using polarized deuteron targets are expected to provide us much more information about the dibaryon states. For example, the measurement of the angular dependence in the backward region would enable us to determine the spin-parity of the resonance unambiguously. We present in Fig. 7 the calculations

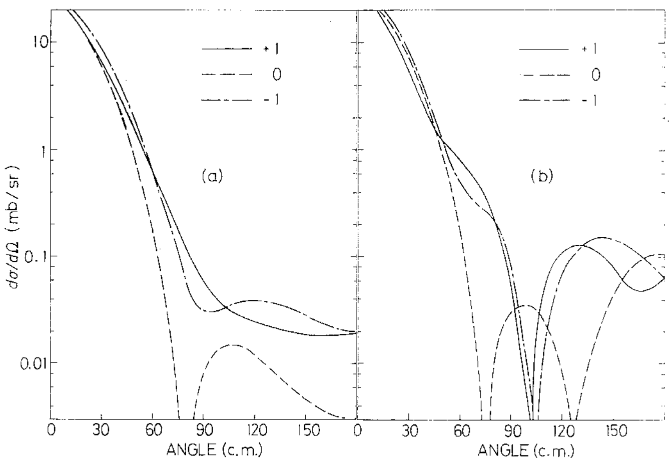

Fig. 7. The angular distribution of πd elastic scattering at 441 MeV/c in case the initial deuteron has definite spin polarization. Figures (a) and (b) show the results of the Glauber model and those with the dibaryon resonances given in Table I, respectively. The quantization axis is taken to be perpendicular to the scattering plane in the laboratory frame.

of the differential cross section for various initial spin orientations with and without the dibaryon resonances.

Acknowledgements

It is a pleasure to thank many people for sharing their knowledge and wisdom with us, without which this work would not have been possible. We would like to express our appreciation to Professor M. Uehara for valuable comments on the dibaryon formation amplitudes, to Professor S. Furuichi for useful discussions on the results of pp phase shift analysis and the dibaryon resonances, to Professor A. Masaike who kindly explained the present status of polarized deuteron targets, and to Professor Y. Oyanagi for helpful discussions regarding πN phase shift analysis. We wish to thank Professor M. Kawaguchi and Professor M. Fukawa for hospitality at National Laboratory of High Energy Physics and to Mr. S. Yashiro for valuable advice and hospitality at the KEK computer center. One of the authors (A.N.) is much indebted to Professor T. Kohmura for helpful discussions on the structure of π-nucleus elastic scattering, and to Professor M. Namiki and Professor S. Ishida for their interest in our work and encouragement. Two of us (K.K. and A.N.) would like to thank the members of the Research group of Young High Energy Physicists in Tokyo (S. Date, I. Hashizume, S. Hirabayashi, N. Suzuki and S. Suzuki) for discussions and encouragement. One (K.K.) and two (A.M. and H.S.) of us acknowledge the financial support of Japan Society for Promotion of Science and National Laboratory of High Energy Physics, respectively. This work was started as one of the Annual Project of the Research Institute for Fundamental Physics in 1977, "Study of High Energy Hadron-Nucleus Interaction".

Appendix

——*Glauber Amplitudes*——

In this appendix we give the explicit form of the Glauber amplitudes in the laboratory frame.

(1) *Single scattering term*

$$T_{11}^{(1)}=(a_{\pi p}+a_{\pi n})\,(\phi_a^{(1)}+\phi_b^{(1)}-\sqrt{2}\,\phi_c^{(1)}+\phi_d^{(1)}/2)\,, \tag{A·1a}$$

$$T_{00}^{(1)}=(a_{\pi p}+a_{\pi n})\,(\phi_a^{(1)}+\phi_b^{(1)}+2\sqrt{2}\,\phi_c^{(1)}-\phi_d^{(1)})\,, \tag{A·1b}$$

$$T_{10}^{(1)}=\{q\,(\tilde{b}_{\pi p}+\tilde{b}_{\pi n})/\sqrt{2}\}\,(-\phi_a^{(1)}+\phi_b^{(1)}/2-\phi_c^{(1)}/\sqrt{2}-\phi_d^{(1)}/2)\,, \tag{A·1c}$$

$$T_{1,-1}^{(1)}=0 \tag{A·1d}$$

and others are given through the relations

$$T_{MM'}^{(1)}=T_{-M,-M'}^{(1)}=T_{M'M}^{(1)}\,. \tag{A·2}$$

Here $\tilde{b}_{\pi N}$ is defined as

$$\tilde{b}_{\pi N} \equiv k \sin\zeta \ b_{\pi N}, \tag{A·3}$$

where k is the beam momentum in the laboratory frame and the amplitudes $a_{\pi N}(\boldsymbol{q})$ and $b_{\pi N}(\boldsymbol{q})$ are given by Eq. (2·5) or (2·6). The form factors are defined as follows:

$$\phi_i^{(1)} \equiv \phi_i(q/2), \quad (i=a, b, c, d) \tag{A·4}$$

where

$$\phi_a(p) = \int_0^\infty dr\ j_0(pr)\,|u(r)|^2, \tag{A·5a}$$

$$\phi_b(p) = \int_0^\infty dr\ j_0(pr)\,|w(r)|^2, \tag{A·5b}$$

$$\phi_c(p) = \int_0^\infty dr\ j_2(pr)\,u(r)\,w(r) \tag{A·5c}$$

and

$$\phi_d(p) = \int_0^\infty dr\ j_2(pr)\,|w(r)|^2. \tag{A·5d}$$

(2) *Double scattering term*

Restricting the two-vector $\boldsymbol{q}'$, which appears in Eq. (2·2), in the x-z plane in the laboratory frame shown in Fig. 1, i.e.,

$$\boldsymbol{q}' = (q'\sin\alpha, 0, q'\cos\alpha), \quad (-\pi<\alpha\leq\pi) \tag{A·6}$$

we get

$$T^{(2)}_{MM'} = \frac{i}{4\pi k}\, 2\int_0^\pi d\alpha \int_0^{q'_{\max}} dq' \mathcal{T}_{MM'}(\boldsymbol{q}, \boldsymbol{q}'), \tag{A·7}$$

where the kinematical boundary is given by

$$q'_{\max} = \frac{1}{2}\left[-q|\cos\alpha| + \{(4+|t^{\pi N}_{\max}|/m_N{}^2)\,|t^{\pi N}_{\max}| - q^2\sin^2\alpha\}^{1/2}\right]. \tag{A·8}$$

Retaining the even part in α, we have

$$\begin{aligned}
\mathcal{T}_{11} = {}& \phi_a{}^{(2)}[A - Bq'^2\sin^2\alpha] \\
& + \phi_b{}^{(2)}[A + B(3q^2 - 12q'^2 - 4q'^2\sin^2\alpha)/40] \\
& - \phi_c{}^{(2)}\sqrt{2}\,[AP_2(\cos\alpha) + B(3q^2+4q'^2)\sin^2\alpha/8] \\
& + \phi_d{}^{(2)}[AP_2(\cos\alpha)/2 + B\{3q^2(7\sin^2\alpha - 2)/112 + q'^2(6+7\sin^2\alpha)/28\}] \\
& + \phi_e{}^{(2)}(3\sqrt{4\pi}/35)\,B[(q^2/4 - q'^2\sin^2\alpha)\{\sqrt{10}\,Y_{42}(\alpha,0) - 2Y_{40}(\alpha,0)\} \\
& - 4q'^2\sin^2\alpha\, Y_{40}(\alpha,0) - 2\sqrt{5}\,q'^2\sin 2\alpha\, Y_{41}(\alpha,0)],
\end{aligned} \tag{A·9a}$$

$$\mathcal{T}_{00}=\phi_a^{(2)}[A+B\{q^2/4+q'^2(1-2\cos^2\alpha)\}]$$
$$+\phi_b^{(2)}[A+B\{q^2-2q'^2(1+\cos^2\alpha)\}/10]$$
$$+\phi_c^{(2)}\sqrt{2}[A\,2P_2(\cos\alpha)+B\{q^2P_2(\cos\alpha)/2-q'^2(1+\cos^2\alpha)\}]$$
$$+\phi_d^{(2)}[-AP_2(\cos\alpha)+B\{q^2(21\sin^2\alpha-8)+4q'^2(1+7\cos^2\alpha)\}/56]$$
$$+\phi_e^{(2)}(6\sqrt{4\pi/35})B[(q^2/4-q'^2\cos^2\alpha)\{2Y_{40}(\alpha,0)-\sqrt{10}Y_{42}(\alpha,0)\}$$
$$+4q'^2\sin^2\alpha Y_{40}(\alpha,0)+2\sqrt{5}q'^2\sin 2\alpha Y_{41}(\alpha,0)], \tag{A·9b}$$

$$\mathcal{T}_{10}=\phi_a^{(2)}[-Gq+H2q'\cos\alpha]$$
$$+\phi_b^{(2)}[Gq/2-Hq'\cos\alpha]$$
$$+\phi_c^{(2)}[-Gq(1-3\sin^2\alpha)/\sqrt{2}+H\sqrt{2}q'\cos\alpha]$$
$$+\phi_d^{(2)}[-Gq(1-3\sin^2\alpha)/2+Hq'\cos\alpha] \tag{A·9c}$$

and

$$\mathcal{T}_{1,-1}=\phi_a^{(2)}B(q^2/4-q'^2\cos^2\alpha)$$
$$+\phi_b^{(2)}B(q^2/4-q'^2\cos^2\alpha)/10$$
$$+\phi_c^{(2)}(1/\sqrt{2})[-A\,3\sin^2\alpha+B\{-q^2P_2(\cos\alpha)/2+q'^2(3-\cos^2\alpha)\}]$$
$$+\phi_d^{(2)}(1/28)[A\,21\sin^2\alpha+B\{q^2(15\sin^2\alpha-4)/4+q'^2(7\cos^2\alpha-3)\}]$$
$$+\phi_e^{(2)}(3\sqrt{4\pi/35})B[(q^2/4-q'^2\cos^2\alpha)\{Y_{40}(\alpha,0)-\sqrt{10}Y_{42}(\alpha,0)$$
$$+\sqrt{70}Y_{44}(\alpha,0)\}-2\sqrt{10}q'^2\sin^2\alpha Y_{42}(\alpha,0)$$
$$+\sqrt{5}\boldsymbol{q'^2}\sin 2\alpha\{Y_{41}(\alpha,0)-\sqrt{7}Y_{43}(\alpha,0)\}], \tag{A·9d}$$

where the form factors are given by

$$\phi_i^{(2)}=\phi_i(q'),\quad (i=a,b,c,d) \tag{A·10}$$

and

$$\phi_e^{(2)}\equiv\phi_e(q')=\int_0^\infty dr\; j_4(q'r)|w(r)|^2. \tag{A·11}$$

The amplitudes A, B, G and H are defined as follows:

$$A=I(a,a), \tag{A·12a}$$
$$B=I(\tilde{b},\tilde{b}), \tag{A·12b}$$
$$G=\{I(a,\tilde{b})+I(\tilde{b},a)\}/2\sqrt{2}, \tag{A·12c}$$
$$H=\{I(a,\tilde{b})-I(\tilde{b},a)\}/2\sqrt{2}, \tag{A·12d}$$

where

$$I(a,\tilde{b})\equiv\{3a_{\pi p}(+)\tilde{b}_{\pi n}(-)+3a_{\pi n}(+)\tilde{b}_{\pi p}(-)$$
$$-a_{\pi p}(+)\tilde{b}_{\pi p}(-)-a_{\pi n}(+)\tilde{b}_{\pi n}(-)\}/4 \qquad (A\cdot 13)$$

with

$$a_{\pi N}(\pm)\equiv a_{\pi N}(\boldsymbol{q}/2\pm\boldsymbol{q}') \qquad (A\cdot 14a)$$

and

$$\tilde{b}_{\pi N}(\pm)\equiv\tilde{b}_{\pi N}(\boldsymbol{q}/2\pm\boldsymbol{q}'). \qquad (A\cdot 14b)$$

In Eqs. (A·9) we have neglected the terms which come from the σ_y component in Eq. (2·5) and in this case we get the relation (A·2) for the double scattering terms.

References

1) F. J. Dyson and N. H. Xuong, Phys. Rev. Letters **13** (1964), 815.
2) V. S. Bhasin and I. M. Duck, Nucl. Phys. **B64** (1973), 289.
3) A. Th. M. Aerts, P. J. G. Mulders and J. J. de Swart, Phys. Rev. **D17** (1978), 260; Phys. Rev. Letters **40** (1978), 1543.
4) S. Furuichi, *A. I. P. Conference Proceedings No. 41, Nucleon-Nucleon Interactions, 1977, Vancouver*, edited by D. F. Measday et al., (American Institute of Physics, New York, 1978), p. 257.
5) T. Kamae and T. Fujita, Phys. Rev. Letters **38** (1977), 471.
6) S. Ishida and M. Oda, Prog. Theor. Phys. **60** (1978), 828.
7) I. Ohba, Waseda University Preprint WU-HEP-78-5 (1978).
8) T. Ueda, Phys. Letters **79B** (1978), 487.
9) L. S. Schroeder et al., Phys. Rev. Letters **27** (1971), 1813.
R. Keller et al., Phys. Rev. **D11** (1975), 2389.
10) T. Kamae et al., Phys. Rev. Letters **38** (1977), 468; Nucl. Phys. **B139** (1978), 394.
11) I. P. Auer et al., Phys. Letters **70B** (1977), 475; Phys. Rev. Letters **41** (1978), 354.
12) K. Hidaka et al., Phys. Letters **70B** (1977), 479.
13) N. Hoshizaki, Prog. Theor. Phys. **58** (1977), 716; **60** (1978), 1796.
14) T. Yao, Phys. Rev. **134** (1964), B454.
15) K. Kanai, A. Minaka, A. Nakamura and H. Sumiyoshi, contributed paper to the 19th International Conference on High Energy Physics, Tokyo, August, 1978.
16) K. Kanai, A. Minaka, A. Nakamura and H. Sumiyoshi, to be published in J. E. T. P. Letters.
17) A. W. Thomas, preprint TRI-PP-77-10 (1977).
18) R. J. Glauber, *Proceedings of the Third International Conference on High Energy Physics and Nuclear Structure* (Plenum press, New York, 1970), p. 207.
19) C. Michael and C. Wilkin, Nucl. Phys. **B11** (1969), 99.
D. P. Sidhu and C. Quigg, Phys. Rev. **D7** (1973), 755.
20) G. Alberi and L. Bertocchi, Nuovo Cim. **63A** (1969), 285.
L. Bertocchi, in *Method in Subnuclear Physics,* (Gordon and Breach, New York, 1969), p. 53.
21) C. Carlson, Phys. Rev. **C2** (1970), 1224.
22) J. M. Wallace, Phys. Rev. **D5** (1972), 1840.
23) A. S. Rinat and A. W. Thomas, Nucl. Phys. **A282** (1977), 365.
24) R. V. Reid, Ann. of Phys. (N.Y.) **50** (1968), 411.
25) M. J. Moravcsik, Nucl. Phys. **7** (1958), 113.
26) E. G. Pewitt et al., Phys. Rev. **131** (1963), 1826.

27) J. H. Norem, Nucl. Phys. **B33** (1971), 512.
28) K. Gabathuler et al., Nucl. Phys. **B55** (1973), 397.
29) R. H. Cole et al., Phys. Rev. **C17** (1978), 681.
30) F. Brandamante et al., Phys. Letters **28B** (1968), 191.
31) M. M. Hoenig, A. S. Rinat, D. Camporese and A. W. Thomas, contributed paper to the 7th International Conference on High Energy Physics and Nuclear Structure, Zurich, 1977.
32) G. Brunhart, G. S. Faughen and V. P. Kenney, Nuovo Cim. **29** (1963), 1162.
33) G. W. Barry, Phys. Rev. **D7** (1973), 1441.